

## ROBUST ANTENNA ARRAY BEAMFORMING UNDER CYCLE FREQUENCY MISMATCH

J.-H. Lee\*

Department of Electrical Engineering, Graduate Institute of Communication Engineering, and Graduate Institute of Biomedical Electronics and Bioinformatics, National Taiwan University, No. 1, Sec. 4, Roosevelt Rd., Taipei 10617, Taiwan

**Abstract**—Many algorithms exploiting the signal cyclostationarity have been shown to be effective in performing antenna array beamforming. However, these algorithms can not provide a unique weight vector for simultaneously extracting multiple signals of interest (SOIs) with distinct cycle frequencies (DCFs). They also suffer from severe performance degradation in the presence of a cycle frequency error (CFE). To simultaneously accommodate multiple SOIs with DCFs and alleviate the effects of cycle leakage due to finite data samples, we propose a cyclic sample matrix inversion (C-SMI) beamformer. To make the C-SMI beamformer robust against CFE, we present a novel objective function which is optimized by using a steepest-descent based algorithm to find the appropriate estimates of the true DCFs. The simulation results show the effectiveness of the robust C-SMI beamformer.

### 1. INTRODUCTION

For conventional adaptive array beamforming, we require the *priori* information of either the impinging direction or the waveform of the desired signal to adapt the weights [1, 2]. A steered-beam beamformer is taught by the actual direction vector of the desired signal and forced to make a constant response in the desired signal direction. Hence, its performance is very sensitive to the accuracy of the steering vector. However, the true direction vector of the desired signal may not be exactly known in some applications, e.g., the application in land mobile-cellular radio systems. Hence, we often encounter the problem

---

*Received 22 August 2011, Accepted 22 October 2011, Scheduled 1 November 2011*

\* Corresponding author: Ju-Hong Lee (juhong@cc.ee.ntu.edu.tw).

of mismatch between the real direction vector of the desired signal and the steering vector. The effectiveness of a steered-beam beamformer can be destroyed even if a small mismatch arises [2, 17–20].

In contrast, adaptive beamforming utilizing signal cyclostationarity has been developed due to two main reasons. Based on the cyclostationary property, we can solve the problem of blind adaptive beamforming, i.e., an adaptive beamformer can automatically preserve the desired signal while cancelling noise and interference without any *priori* information about the desired signal direction [3]. Moreover, cyclostationarity is a statistical property possessed by most of practical man-made communication signals [4, 5]. Another cyclic adaptive beamforming (CAB) algorithm and two more complicated CAB-based algorithms, namely, the constrained CAB (C-CAB) and the robust CAB (R-CAB), were also proposed in [6] to enhance the performance of the CAB algorithm. However, these three algorithms are eigenvalue problems and work for extracting either one signal of interest (SOI) or multiple SOIs with the same cycle frequency. For multiple SOIs having distinct cycle frequencies (DCF), they treat each SOI as a single signal. It has been shown in [6] that the least-squares spectral self-coherence restoral (LS-SCORE) and C-CAB algorithms have the same asymptotical maximum output signal-to-interference plus noise ratio (SINR) performance as the number of data snapshots approaches infinite. Among these blind beamforming techniques, the LS-SCORE approach [3] has been extensively considered [7] because of its simplicity in avoiding the computationally expensive eigen-decomposition or singular-value decomposition (SVD) in implementation. The *priori* information that the original LS-SCORE approach requires to work is only the cycle frequency of the SOI. Hence, its performance is sensitive to the accuracy of the presumed cycle frequency. However, the actual cycle frequency of the SOI may not be known exactly in some applications due, for example, to the phenomenon of Doppler shift. The research work in [8, 9] has presented an analytical formula that demonstrates the behavior of the performance degradation due to cycle frequency error (CFE) for the LS-SCORE approach. The output SINR of an adaptive blind beamformer using the LS-SCORE approach deteriorates like a sinc function as the number of data snapshots increases. Robust approaches based on the LS-SCORE algorithm were then presented in [8, 9] for estimating the true cycle frequency. Recently, three robust algorithms based on the CAB algorithm of [6] were developed in [10] to deal with CFE. The subspace constrained CAB (SC-CAB) algorithm simply projects the CAB weight vector onto the signal-plus-interference subspace to alleviate the steering vector error due to CFE. The robust SC-CAB algorithm is a combination of the SC-CAB algo-

rithm and the robust idea based on optimization of worst-case performance [11]. A convex second-order cone optimization problem with an optimal value of the diagonal loading factor must be solved under the uncertainty of the SC-CAB weight vector. The structured steering vector (SSV) algorithm estimates the direction vector of the SOI from the SC-CAB weight vector. Then it finds the SSV weight vector by minimizing the array output power with a distortionless constraint towards the estimated SOI's direction vector. These three robust algorithms work for extracting either only one SOI or multiple SOIs with the same cycle frequency. Besides these three CAB-based robust algorithms are still eigenvalue problems, they cannot provide a unique weight vector for simultaneously receiving multiple SOIs with DCFs.

In this paper, we consider adaptive blind beamforming under multiple SOIs with DCFs. To simultaneously accommodate multiple SOIs with DCFs and alleviate the effects of cycle leakage due to finite data samples, a cyclic sample matrix inversion (C-SMI) beamformer which is developed based on the conventional SMI beamformer with the exploitation of signal cyclostationarity and diagonal loading. To make the C-SMI beamformer robust against CFE, we present a novel objective function to formulate an optimization problem. The true DCFs can be estimated by solving the optimization problem through a steepest-descent based iterative algorithm with the exploitation of signal cyclostationarity. The C-SMI beamformer with the iterative algorithm effectively provides a weight vector for simultaneously extracting multiple SOIs with DCFs against CFE.

This paper is organized as follows. In Section 2, we briefly describe the original LS-SCORE algorithm of [3]. The C-SMI beamformer for adaptive blind beamforming under multiple SOIs with DCFs is presented in Section 3. We present the theoretical work for alleviating the performance degradation caused by the CFE in Section 4. The convergence analysis of the proposed approach is presented in Section 5. Several computer simulation examples for confirming the effectiveness of the proposed approach are provided in Section 6. Finally, we conclude the paper in Section 7.

## 2. CONVENTIONAL ADAPTIVE BEAMFORMING USING CYCLOSTATIONARITY

### 2.1. Signal Cyclostationarity

Cyclostationarity is a statistical property possessed by most of practical man-made communication signals. A signal  $r(t)$  with cyclostationarity has the property that its cyclic correlation function (CCF) and cyclic conjugate correlation function (CCCF) given by the

following infinite time averages

$$\begin{aligned} \mathbf{R}_{rr}(\alpha, \tau) &= \langle r(t)r^*(t-\tau)e^{-j2\pi\alpha t} \rangle_\infty \\ \text{and } \mathbf{R}_{rr^*}(\alpha, \tau) &= \langle r(t)r(t-\tau)e^{-j2\pi\alpha t} \rangle_\infty \end{aligned} \quad (1)$$

respectively, are not equal to zero at some time delay  $\tau$  and cycle frequency  $\alpha$ , where the superscript “\*” denotes the complex conjugate. It has been shown in [9] that many modulated signals exhibit cyclostationarity with cycle frequency equal to twice the carrier frequency or multiples of the baud rate or combinations of these. For the data vector  $\mathbf{x}(t)$  received by an antenna array with  $N$  isotropic sensor elements, the associated cyclic correlation matrix (CCM) and cyclic conjugate correlation matrix (CCCM) are given by

$$\begin{aligned} \mathbf{R}_{\mathbf{xx}}(\alpha, \tau) &= \langle \mathbf{x}(t)\mathbf{x}^H(t-\tau)e^{-j2\pi\alpha t} \rangle_\infty \\ \text{and } \mathbf{R}_{\mathbf{xx}^*}(\alpha, \tau) &= \langle \mathbf{x}(t)\mathbf{x}^T(t-\tau)e^{-j2\pi\alpha t} \rangle_\infty, \end{aligned} \quad (2)$$

respectively, where the superscripts “ $H$ ” and “ $T$ ” denote the conjugate transpose and the complex conjugate, respectively.

## 2.2. Conventional Adaptive Beamforming Using Signal Cyclostationarity

Consider an adaptive beamformer using an  $M$ -element antenna array excited by a signal of interest (SOI),  $J$  interferers, and spatially white noise. The received data vector  $\mathbf{x}(t)$  is given by

$$\mathbf{x}(t) = s(t)\mathbf{a}(\theta_d) + \sum_{j=1}^J s_j(t)\mathbf{a}(\theta_j) + \mathbf{n}(t) = s(t)\mathbf{a}(\theta_d) + \mathbf{i}(t), \quad (3)$$

where  $s(t)$  and  $s_j(t)$  denotes the waveforms of the SOI and the  $j$ th interferer,  $\mathbf{a}(\theta_d)$  and  $\mathbf{a}(\theta_j)$  the direction vectors of the SOI with direction angle  $\theta_d$  and the  $j$ th interferer with direction angle  $\theta_j$ , and  $\mathbf{n}(t)$  the noise vector, respectively. The array output is given by  $y(t) = \mathbf{w}^H \mathbf{x}(t)$ , where  $\mathbf{w}$  denotes the weight vector of the beamformer. Assume that  $s(t)$  is cyclostationary and has a cycle frequency  $\alpha$ , but  $\mathbf{i}(t)$  is not cyclostationary at  $\alpha$  and is temporally uncorrelated with  $s(t)$ . According to the original LS-SCORE algorithm of [3], a cost function is defined as follows:

$$G(\mathbf{w}; \mathbf{c}) = \langle |y(t) - r(t)|^2 \rangle_T, \quad (4)$$

where the reference signal  $r(t)$  is given by

$$r(t) = \mathbf{c}^H \mathbf{x}^*(t-\tau)e^{j2\pi\alpha t} \quad (5)$$

and  $\langle \cdot \rangle_T$  denotes the average over the time interval  $[0, T]$ .  $\mathbf{c}$  is a fixed control vector. The optimal weight vector  $\mathbf{w}_{ls}$  minimizing (4) is given by [3]

$$\mathbf{w}_{ls} = \hat{\mathbf{R}}_{\mathbf{xx}}^{-1} \hat{\mathbf{r}}_{\mathbf{xr}}(\alpha), \tag{6}$$

where  $\hat{\mathbf{R}}_{\mathbf{xx}} = \langle \mathbf{x}(t)\mathbf{x}^H(t) \rangle_T$  and  $\hat{\mathbf{r}}_{\mathbf{xr}}(\alpha) = \langle \mathbf{x}(t)r^*(t) \rangle_T$  are the sample correlation matrix of  $\mathbf{x}(t)$  and the sample cross-correlation vector of  $\mathbf{x}(t)$  and  $r(t)$  computed over  $[0, T]$ , respectively. For any control vector  $\mathbf{c}$  as long as  $\mathbf{c}^H \mathbf{a}(\theta_d) \neq 0$ , it is shown in [3] that (6) converges to the solution of conventional adaptive beamforming based on the maximum output SINR criterion as  $T$  approaches infinite.

### 3. ADAPTIVE BLIND BEAMFORMING WITH MULTIPLE CYCLE FREQUENCIES

Assume that there are  $D$  uncorrected SOIs with direction angles  $\theta_d$  and DCFs  $\alpha_d, d = 1, 2, \dots, D$  and  $J$  interferers. The received data vector  $\mathbf{x}(t)$  becomes

$$\mathbf{x}(t) = \sum_{d=1}^D s_d(t)\mathbf{a}(\theta_d) + \sum_{j=D+1}^{D+J} s_j(t)\mathbf{a}(\theta_j) + \mathbf{n}(t) = \sum_{d=1}^D s_d(t)\mathbf{a}(\theta_d) + \mathbf{i}(t). \tag{7}$$

To accommodate the  $D$  SOIs, we use the following reference signal

$$r(\alpha_1, \alpha_2, \dots, \alpha_D; t) = \sum_{d=1}^D e^{j2\pi\alpha_d t} \mathbf{c}^H \mathbf{x}^*(t - \tau). \tag{8}$$

Let the interferers and noise do not have the cycle frequencies equal to  $\alpha_d, d = 1, 2, \dots, D$ . It is shown in Appendix A that the corresponding  $\hat{\mathbf{r}}_{\mathbf{xr}}(\alpha_1, \alpha_2, \dots, \alpha_D) = \langle \mathbf{x}(t)r^*(\alpha_1, \alpha_2, \dots, \alpha_D; t) \rangle_T$  approaches  $\mathbf{r}_{\mathbf{xr}}(\alpha_1, \alpha_2, \dots, \alpha_D) = \sum_{d=1}^D \{\text{trace}\{\mathbf{R}_{\mathbf{xx}}(\alpha_d, 0)\} \rho_{s_d s_d^*}(\alpha_d, 0) / \{M \rho_{s_d s_d}(\alpha_d, 0)\}\} \mathbf{a}(\theta_d)$  as  $T$  approaches infinity, where  $\rho_{s_d s_d}(\alpha_d, 0)$  and  $\rho_{s_d s_d^*}(\alpha_d, 0)$  denote the cyclic correlation coefficient (CCC) and cyclic conjugate correlation coefficient (CCCC) of  $s_d(t)$  computed at  $\tau = 0$ , respectively. As a result,  $\hat{\mathbf{r}}_{\mathbf{xr}}(\alpha_1, \alpha_2, \dots, \alpha_D)$  can be used as a weight vector to retrieve the  $D$  SOIs. However, the effects of cycle leakage due to finite data samples as shown by [8, 9] will be significant if we directly set the beamformer’s weight vector equal to  $\hat{\mathbf{r}}_{\mathbf{xr}}(\alpha_1, \alpha_2, \dots, \alpha_D)$ . To alleviate the effects of cycle leakage, we propose an approach based on the results

of Appendix A. First, the CCC and CCCC of  $s_d(t)$  are given as follows [12, 13] :

$$\rho_{s_d s_d}(\alpha_d, \tau) = \frac{\mathbf{R}_{s_d s_d}(\alpha_d, \tau)}{\mathbf{r}_{s_d s_d}} \text{ and } \rho_{s_d s_d^*}(\alpha_d, \tau) = \frac{\mathbf{R}_{s_d s_d^*}(\alpha_d, \tau)}{\mathbf{r}_{s_d s_d}}, \quad (9)$$

respectively, where  $r_{s_d s_d}$  denotes the average power of  $s_d(t)$ . For a given cyclostationary signal  $s_d(t)$ , its  $\rho_{s_d s_d}(\alpha_d, \tau)$  and  $\rho_{s_d s_d^*}(\alpha_d, \tau)$  can be computed in advance. Using (9) and (A4), we obtain the average power of  $s_d(t)$  as follows:

$$r_{s_d s_d} = \frac{\text{trace}\{\mathbf{R}_{\mathbf{xx}}(\alpha_d, \tau)\}}{M \rho_{s_d s_d}(\alpha_d, \tau)}. \quad (10)$$

Moreover, the CCCC  $R_{s_d s_d^*}(\alpha_d, \tau)$  of  $s_d(t)$  can be obtained from (9) and (10) as follows:

$$R_{s_d s_d^*}(\alpha_d, \tau) = \rho_{s_d s_d^*}(\alpha_d, \tau) \times \frac{\text{trace}\{\mathbf{R}_{\mathbf{xx}}(\alpha_d, \tau)\}}{M \rho_{s_d s_d}(\alpha_d, \tau)}. \quad (11)$$

Therefore, the correlation matrix  $\mathbf{R}_{ss}$  due to the  $D$  uncorrected SOIs can be expressed as

$$\begin{aligned} \mathbf{R}_{ss} &= E \left\{ \left( \sum_{d=1}^D s_d(t) \mathbf{a}(\theta_d) \right) \left( \sum_{d=1}^D s_d(t) \mathbf{a}(\theta_d) \right)^H \right\} \\ &= \sum_{d=1}^D r_{s_d s_d} \mathbf{a}(\theta_d) \mathbf{a}(\theta_d)^H. \end{aligned} \quad (12)$$

Based on (A6) of Appendix A, we can obtain  $\mathbf{a}(\theta_d)$  as follows:

$$\mathbf{a}(\theta_d) = \rho_{s_d s_d}(\alpha_d, 0) M \mathbf{r}_{\mathbf{xr}}(\alpha_d) / \{ \text{trace}\{\mathbf{R}_{\mathbf{xx}}(\alpha_d, 0)\} \rho_{s_d s_d^*}(\alpha_d, 0) \}. \quad (13)$$

Therefore, we note from (13) that  $\hat{\mathbf{r}}_{\mathbf{xr}}(\alpha_d)$  can be viewed as a consistent estimate of  $\mathbf{a}(\theta_d)$ . In case of finite data samples, we can set the estimate  $\hat{\mathbf{a}}(\theta_d)$  of  $\mathbf{a}(\theta_d)$  equal to the normalized version of  $\hat{\mathbf{r}}_{\mathbf{xr}}(\alpha_d)$ , i.e.,  $\hat{\mathbf{a}}(\theta_d) = \hat{\mathbf{r}}_{\mathbf{xr}}(\alpha_d) / (\hat{r}_{\mathbf{xr}}(1) \sqrt{M})$ , where  $\hat{r}_{\mathbf{xr}}(1)$  denotes the first element of  $\hat{\mathbf{r}}_{\mathbf{xr}}(\alpha_d)$ . Substituting (13) into (12) yields

$$\begin{aligned} \mathbf{R}_{ss} &= \sum_{d=1}^D \frac{\text{trace}\{\mathbf{R}_{\mathbf{xx}}(\alpha_d, 0)\}}{M \rho_{s_d s_d}(\alpha_d, 0)} \{ \rho_{s_d s_d}(\alpha_d, 0) M \mathbf{r}_{\mathbf{xr}}(\alpha_d) \\ &\quad / \{ \text{trace}\{\mathbf{R}_{\mathbf{xx}}(\alpha_d, 0)\} \rho_{s_d s_d^*}(\alpha_d, 0) \} \} \times \{ \rho_{s_d s_d}(\alpha_d, 0) M \mathbf{r}_{\mathbf{xr}}(\alpha_d) \\ &\quad / \{ \text{trace}\{\mathbf{R}_{\mathbf{xx}}(\alpha_d, 0)\} \rho_{s_d s_d^*}(\alpha_d, 0) \} \}^H. \end{aligned} \quad (14)$$

The correlation matrix  $\mathbf{R}_{\text{ii}}$  due to the interference plus noise can be obtained as follows:

$$\begin{aligned} \mathbf{R}_{\text{ii}} &= \mathbf{R}_{\text{xx}} - \mathbf{R}_{\text{ss}} \\ &= E\{\mathbf{x}(t)\mathbf{x}(t)^H\} - \sum_{d=1}^D \frac{\text{trace}\{\mathbf{R}_{\text{xx}}(\alpha_d, 0)\}}{M\rho_{s_d s_d}(\alpha_d, 0)} \{\rho_{s_d s_d}(\alpha_d, 0)M\mathbf{r}_{\text{xr}}(\alpha_d) \\ &\quad / \{\text{trace}\{\mathbf{R}_{\text{xx}}(\alpha_d, 0)\}\rho_{s_d s_d^*}(\alpha_d, 0)\}\} \times \{\rho_{s_d s_d}(\alpha_d, 0)M\mathbf{r}_{\text{xr}}(\alpha_d) \\ &\quad / \{\text{trace}\{\mathbf{R}_{\text{xx}}(\alpha_d, 0)\}\rho_{s_d s_d^*}(\alpha_d, 0)\}\}^H. \end{aligned} \quad (15)$$

The above procedure proposed for obtaining  $\mathbf{R}_{\text{ii}}$  does not need to solve any eigenvalue problem. In contrast, the R-CAB algorithm [6] based on the C-CAB algorithm does need to solve an eigenvalue problem for computing  $\mathbf{R}_{\text{ii}}$ .

To compute an efficient weight vector  $\mathbf{w}_{\text{new}}$  for simultaneously receiving multiple cyclostationary signals with DCFs, we combine the sample matrix inversion (SMI) beamformer [1] with the exploitation of signal cyclostationarity and the diagonal loading (DL) [14] as follows:

$$\hat{\mathbf{w}}_{\text{new}} = (\hat{\mathbf{R}}_{\text{ii}} + \kappa\mathbf{I})^{-1}\hat{\mathbf{r}}_{\text{xr}}(\alpha_1, \alpha_2, \dots, \alpha_D), \quad (16)$$

where  $\hat{\mathbf{R}}_{\text{ii}}$  denotes the sample version of  $\mathbf{R}_{\text{ii}}$  computed by taking the data samples over the time interval  $[0, T]$ ,  $\mathbf{I}$  the  $M \times M$  identity matrix, and  $\hat{\mathbf{w}}_{\text{new}}$  the sample version of  $\mathbf{w}_{\text{new}} = (\mathbf{R}_{\text{ii}} + \kappa\mathbf{I})^{-1}\mathbf{r}_{\text{xr}}(\alpha_1, \alpha_2, \dots, \alpha_D)$ . We term the beamformer with the weight vector of (16) as the cyclic SMI (C-SMI) beamformer. Since the noise eigenvalues associated with  $\hat{\mathbf{R}}_{\text{ii}}$  show random variation due to the finite sample data, the noise eigenvectors affect the SMI beamformer's response in a manner determined by the variation of the corresponding random eigenvalues. As a result, a conventional SMI beamformer suffers from the addition of randomly weighted noise eigenvectors and hence higher sidelobe level in its adaptive beam pattern. Adding the loading factor  $\kappa$  in (16) is to add the loading level to all the eigenvalues associated with  $\hat{\mathbf{R}}_{\text{ii}}$  and hence produces a bias in the noise eigenvalues to reduce their random variation. To enhance the performance of the C-SMI beamformer, the loading factor  $\kappa$  is usually chosen according to the power level of the SOIs. According to our simulation experience, it is appropriate to set  $\kappa$  to a large value so that  $\kappa\mathbf{I}$  dominates the term  $(\hat{\mathbf{R}}_{\text{ii}} + \kappa\mathbf{I})$  when the  $D$  SOIs are strong. In contrast,  $\kappa$  is set to a small value so that  $\hat{\mathbf{R}}_{\text{ii}}$  dominates when the  $D$  SOIs are weak. Hence, an appropriate choice for  $\kappa$  is given by

$$\kappa = \text{trace}\left\{\hat{\mathbf{R}}_{\text{ss}}\right\}, \quad (17)$$

where  $\hat{\mathbf{R}}_{ss}$  denotes the sample version of  $\mathbf{R}_{ss}$  computed over the time interval  $[0, T]$ . Recently, an ad-hoc way developed for conventional standard Capon beamformer to determine the loading factor level was presented in [16].

To make a comparison between the proposed C-SMI beamformer and the LS-SCORE beamformer for simultaneously receiving multiple cyclostationary signals with DCFs, we modify the original LS-SCORE weight vector of (6) by replacing the  $\hat{\mathbf{r}}_{xr}(\alpha)$  with  $\hat{\mathbf{r}}_{xr}(\alpha_1, \alpha_2, \dots, \alpha_D)$ , i.e., the weight vector is set to  $\mathbf{w}_{ls} = \hat{\mathbf{R}}_{xx}^{-1} \hat{\mathbf{r}}_{xr}(\alpha_1, \alpha_2, \dots, \alpha_D)$ .

#### 4. ROBUST BLIND BEAMFORMING AGAINST CFE

Here, we present a robust approach for performing blind beamforming against CFE. First, consider the concept for conventional linearly constrained minimum variance (LCMV) beamforming with main-beam constraint [1]. The optimum weight vector  $\hat{\mathbf{w}}_{LCMV}$  is obtained by minimizing the array output power subject to the steered-beam constraint as follows:

$$\text{Minimize } \hat{\mathbf{w}}_{LCMV}^H \hat{\mathbf{R}}_{xx} \hat{\mathbf{w}}_{LCMV} \quad \text{Subject to } \hat{\mathbf{w}}_{LCMV} \mathbf{a}(\theta_d) = 1, \quad (18)$$

where  $\theta_d$  is the SOI's direction angle. It is easy to show that the minimum value of  $\hat{\mathbf{w}}_{LCMV}^H \hat{\mathbf{R}}_{xx} \hat{\mathbf{w}}_{LCMV}$  corresponding to the optimum solution of  $\hat{\mathbf{w}}_{LCMV}$  is equal to the inverse of  $\mathbf{a}(\theta_d)^H \hat{\mathbf{R}}_{xx}^{-1} \mathbf{a}(\theta_d)$ . Using this result and (A6) of Appendix A, we propose an objective function  $Q(\hat{\alpha}_1, \hat{\alpha}_2, \dots, \hat{\alpha}_D)$  for the considered problem as follows:

$$Q(\hat{\alpha}_1, \hat{\alpha}_2, \dots, \hat{\alpha}_D) = \hat{\mathbf{r}}_{xr}(\hat{\alpha}_1, \hat{\alpha}_2, \dots, \hat{\alpha}_D)^H \hat{\mathbf{R}}_{xx}^{-1} \hat{\mathbf{r}}_{xr}(\hat{\alpha}_1, \hat{\alpha}_2, \dots, \hat{\alpha}_D), \quad (19)$$

where  $\hat{\alpha}_1, \hat{\alpha}_2, \dots$ , and  $\hat{\alpha}_D$  represent the estimates of  $\alpha_1, \alpha_2, \dots$ , and  $\alpha_D$ , respectively. Clearly, this objective function reaches its maximum when the estimates  $\hat{\alpha}_1, \hat{\alpha}_2, \dots, \hat{\alpha}_D$  are equal to the actual  $\alpha_1, \alpha_2, \dots, \alpha_D$ , respectively. To find the appropriate estimates for the DCFs  $\alpha_1, \alpha_2, \dots, \alpha_D$ , we formulate the following optimization problem:

$$\text{Maximize } \hat{\mathbf{r}}_{xr}(\hat{\alpha}_1, \hat{\alpha}_2, \dots, \hat{\alpha}_D)^H \hat{\mathbf{R}}_{xx}^{-1} \hat{\mathbf{r}}_{xr}(\hat{\alpha}_1, \hat{\alpha}_2, \dots, \hat{\alpha}_D), \quad (20)$$

$$\hat{\alpha}_1, \hat{\alpha}_2, \dots, \hat{\alpha}_D$$

To solve (20), we adapt the method of steepest descent by taking the derivatives of the objective function  $Q(\hat{\alpha}_1, \hat{\alpha}_2, \dots, \hat{\alpha}_D)$  with respect to

$\hat{\alpha}_1, \hat{\alpha}_2, \dots, \hat{\alpha}_D$ . The derivatives are given by

$$\begin{aligned} \nabla_{\hat{\alpha}_d} Q(\hat{\alpha}_1, \hat{\alpha}_2, \dots, \hat{\alpha}_D) &= \frac{\partial Q(\hat{\alpha}_1, \hat{\alpha}_2, \dots, \hat{\alpha}_D)}{\partial \hat{\alpha}_d} \\ &= \frac{\partial \hat{\mathbf{r}}_{\mathbf{x}r}(\hat{\alpha}_1, \hat{\alpha}_2, \dots, \hat{\alpha}_D)^H \hat{\mathbf{R}}_{\mathbf{xx}}^{-1} \hat{\mathbf{r}}_{\mathbf{x}r}(\hat{\alpha}_1, \hat{\alpha}_2, \dots, \hat{\alpha}_D)}{\partial \hat{\alpha}_d} \\ &= \frac{\partial \hat{\mathbf{r}}_{\mathbf{x}r}(\hat{\alpha}_1, \hat{\alpha}_2, \dots, \hat{\alpha}_D)^H}{\partial \hat{\alpha}_d} \hat{\mathbf{R}}_{\mathbf{xx}}^{-1} \hat{\mathbf{r}}_{\mathbf{x}r}(\hat{\alpha}_1, \hat{\alpha}_2, \dots, \hat{\alpha}_D) \\ &\quad + \hat{\mathbf{r}}_{\mathbf{x}r}(\hat{\alpha}_1, \hat{\alpha}_2, \dots, \hat{\alpha}_D)^H \hat{\mathbf{R}}_{\mathbf{xx}}^{-1} \frac{\partial \hat{\mathbf{r}}_{\mathbf{x}r}(\hat{\alpha}_1, \hat{\alpha}_2, \dots, \hat{\alpha}_D)}{\partial \hat{\alpha}_d} \\ &= 2 \times \text{real} \left\{ \hat{\mathbf{r}}_{\mathbf{x}r}(\hat{\alpha}_1, \hat{\alpha}_2, \dots, \hat{\alpha}_D)^H \hat{\mathbf{R}}_{\mathbf{xx}}^{-1} \frac{\partial \hat{\mathbf{r}}_{\mathbf{x}r}(\hat{\alpha}_1, \hat{\alpha}_2, \dots, \hat{\alpha}_D)}{\partial \hat{\alpha}_d} \right\} \\ &= 2 \times \text{real} \left\{ \hat{\mathbf{r}}_{\mathbf{x}r}(\hat{\alpha}_1, \hat{\alpha}_2, \dots, \hat{\alpha}_D)^H \hat{\mathbf{R}}_{\mathbf{xx}}^{-1} \hat{\mathbf{r}}_{\mathbf{x}u_d}(\hat{\alpha}_d) \right\}, \end{aligned} \tag{21}$$

for  $d = 1, 2, \dots, D$ , where

$$\begin{aligned} \hat{\mathbf{r}}_{\mathbf{x}u_d}(\hat{\alpha}_d) &= \partial \langle \mathbf{x}(t) r^*(\hat{\alpha}_1, \hat{\alpha}_2, \dots, \hat{\alpha}_D; t) \rangle_T / \partial \hat{\alpha}_d \\ &= \left\langle \mathbf{x}(t) \mathbf{x}^T(t) \mathbf{c} e^{-j2\pi\hat{\alpha}_d t} (-j2\pi t) \right\rangle_T. \end{aligned} \tag{22}$$

Since the objective function  $Q(\hat{\alpha}_1, \hat{\alpha}_2, \dots, \hat{\alpha}_D)$  reaches the maximum at  $\alpha_1, \alpha_2, \dots, \alpha_D$ , it should be approximately a concave function in an appropriate neighborhood of  $\alpha_1, \alpha_2, \dots, \alpha_D$ . Accordingly, the updated value of the estimate for the cycle frequency  $\alpha_d$  at the time instant  $t_{i+1}$  can be computed by using the following recursive formula:

$$\begin{aligned} \hat{\alpha}_d(t_{i+1}) &= \hat{\alpha}_d(t_i) + \nu_d(t_i) \nabla_{\hat{\alpha}_d} Q(\hat{\alpha}_1, \hat{\alpha}_2, \dots, \hat{\alpha}_D) \\ \hat{\alpha}_1 &= \hat{\alpha}_1(t_i), \hat{\alpha}_2 = \hat{\alpha}_2(t_i), \dots, \hat{\alpha}_D = \hat{\alpha}_D(t_i), \end{aligned} \tag{23}$$

for  $d = 1, 2, \dots, D$ , where  $\nu_d(t_i)$  is a positive real-valued parameter referred to as the step-size parameter. Examining the derivatives given by (21), we set the step-size parameter equal to

$$\nu_d(t_i) = \frac{1}{\left\| \left\langle \mathbf{x}(t) \mathbf{x}^T(t) e^{-j2\pi\hat{\alpha}_d(t_i)t} (-j2\pi t) \right\rangle_{t_i} \right\|^{p_d}} \tag{24}$$

for  $d = 1, 2, \dots, D$ , to ensure the convergence of the steepest-descent based algorithm used by (23), where  $\|\mathbf{B}\|$  denotes the maximum singular value of the matrix  $\mathbf{B}$ . As shown in the next section,  $p_d$  is a positive real value which must be appropriately determined to ensure the convergence. The updated weight vector at the time instant  $t_{i+1}$  is obtained by substituting (23) into (16) and given by

$$\hat{\mathbf{w}}_{\text{new}}(t_{i+1}) = \left( \hat{\mathbf{R}}_{\text{ii}}(t_{i+1}) + \kappa \mathbf{I} \right)^{-1} \hat{\mathbf{r}}_{\mathbf{x}r}(\hat{\alpha}_1(t_{i+1}), \hat{\alpha}_2(t_{i+1}), \dots, \hat{\alpha}_D(t_{i+1})), \tag{25}$$

where  $\hat{\mathbf{R}}_{\mathbf{ii}}(t_{i+1})$  denotes the sample version of  $\mathbf{R}_{\mathbf{ii}}$  computed in the time interval  $[0, t_{i+1}]$  with  $t_{i+1} = (i+1)T_s$  and the sampling period =  $T_s$ .

## 5. CONVERGENCE OF THE PROPOSED APPROACH

From (19), we can obtain the following expression after some algebraic manipulations

$$\begin{aligned} Q(\hat{\alpha}_1(t_i), \hat{\alpha}_2(t_i), \dots, \hat{\alpha}_D(t_i)) &= \hat{\mathbf{r}}_{\mathbf{x}r}(\hat{\alpha}_1(t_i), \hat{\alpha}_2(t_i), \dots, \hat{\alpha}_D(t_i))^H \hat{\mathbf{R}}_{\mathbf{xx}}^{-1}(t_i) \\ \hat{\mathbf{r}}_{\mathbf{x}r}(\hat{\alpha}_1(t_i), \hat{\alpha}_2(t_i), \dots, \hat{\alpha}_D(t_i)) &= \frac{1}{i^2} \sum_{l=0}^{i-1} \sum_{k=0}^{i-1} \sum_{u=1}^D \sum_{v=1}^D \left\{ \mathbf{c}^H \mathbf{x}^*(l) \mathbf{x}^T(k) \mathbf{c} \right\} \\ &\times \left\{ \mathbf{x}^H(l) \hat{\mathbf{R}}_{\mathbf{xx}}^{-1}(t_i) \mathbf{x}(k) \right\} e^{j2\pi(l\hat{\alpha}_u - k\hat{\alpha}_v)T_s}, \end{aligned} \quad (26)$$

where we add the time index  $t_i$  to indicate that the objective function is computed at the time instant  $t_i$ . From (7), the term  $\mathbf{x}^H(l) \hat{\mathbf{R}}_{\mathbf{xx}}^{-1}(t_i) \mathbf{x}(k)$  can be approximated as follows:

$$\begin{aligned} \mathbf{x}^H(l) \hat{\mathbf{R}}_{\mathbf{xx}}^{-1}(t_i) \mathbf{x}(k) &\approx \sum_{d=1}^D s_d^*(l) s_d(k) \left\{ \mathbf{a}(\theta_d)^H \hat{\mathbf{R}}_{\mathbf{xx}}^{-1}(t_i) \mathbf{a}(\theta_d) \right\} \\ &+ \sum_{j=D+1}^{D+J} s_j^*(l) s_j(k) \left\{ \mathbf{a}(\theta_j)^H \hat{\mathbf{R}}_{\mathbf{xx}}^{-1}(t_i) \mathbf{a}(\theta_j) \right\} + \text{noise-related terms.} \end{aligned} \quad (27)$$

(27) is obtained due to  $\mathbf{a}(\theta_d)^H \hat{\mathbf{R}}_{\mathbf{xx}}^{-1}(t_i) \mathbf{a}(\theta_j) \approx 0$  and  $\mathbf{a}(\theta_j)^H \hat{\mathbf{R}}_{\mathbf{xx}}^{-1}(t_i) \mathbf{a}(\theta_j) \approx 0$  as the number  $i$  of data snapshots approaches infinity,  $j, \bar{j} = D+1, 2, \dots, D+J$  and  $j \neq \bar{j}$ . The term  $\mathbf{c}^H \mathbf{x}^*(l) \mathbf{x}^T(k) \mathbf{c}$  can be expressed as follows:

$$\begin{aligned} \mathbf{c}^H \mathbf{x}^*(l) \mathbf{x}^T(k) \mathbf{c} &= \mathbf{c}^H \left\{ \sum_{d=1}^D s_d(l) \mathbf{a}(\theta_d) + \sum_{j=1}^J s_j(l) \mathbf{a}(\theta_j) + \mathbf{n}(l) \right\}^* \\ &\left\{ \sum_{d=1}^D s_d(k) \mathbf{a}(\theta_d) + \sum_{j=D+1}^{D+J} s_j(k) \mathbf{a}(\theta_j) + \mathbf{n}(k) \right\}^T \mathbf{c} \\ &= \sum_{d=1}^D s_d^*(l) s_d(k) \left\{ \mathbf{c}^H \mathbf{a}^*(\theta_d) \mathbf{a}^T(\theta_d) \mathbf{c} \right\} + \sum_{j=D+1}^{D+J} s_j^*(l) s_j(k) \\ &\left\{ \mathbf{c}^H \mathbf{a}^*(\theta_j) \mathbf{a}^T(\theta_j) \mathbf{c} \right\} + \left\{ \mathbf{c}^H \mathbf{n}^*(l) \mathbf{n}^T(k) \mathbf{c} \right\} + \text{cross terms.} \end{aligned} \quad (28)$$

We have from (27) and (28) that

$$\begin{aligned}
 & \left\{ \mathbf{c}^H \mathbf{x}^*(l) \mathbf{x}^T(k) \mathbf{c} \right\} \left\{ \mathbf{x}^H(l) \hat{\mathbf{R}}_{\mathbf{xx}}^{-1}(t_i) \mathbf{x}(k) \right\} \\
 & \approx \sum_{d=1}^D s_d^*(l) s_d^*(l) s_d(k) s_d(k) \left\{ \mathbf{a}(\theta_d)^H \hat{\mathbf{R}}_{\mathbf{xx}}^{-1}(t_i) \mathbf{a}(\theta_d) \right\} \left\{ \mathbf{c}^H \mathbf{a}^*(\theta_d) \mathbf{a}^T(\theta_d) \mathbf{c} \right\} \\
 & + \sum_{j=D+1}^{D+J} s_j^*(l) s_j^*(l) s_j(k) s_j(k) \left\{ \mathbf{a}(\theta_j)^H \hat{\mathbf{R}}_{\mathbf{xx}}^{-1}(t_i) \mathbf{a}(\theta_j) \right\} \left\{ \mathbf{c}^H \mathbf{a}^*(\theta_j) \mathbf{a}^T(\theta_j) \mathbf{c} \right\} \\
 & + \text{the cross terms including noise and interference.} \tag{29}
 \end{aligned}$$

As the number  $i$  of data snapshots approaches infinity, we substitute (29) into (26) and perform some necessary algebraic manipulations to obtain

$$\begin{aligned}
 Q(\hat{\alpha}_1(t_i), \hat{\alpha}_2(t_i), \dots, \hat{\alpha}_D(t_i)) &= \hat{\mathbf{r}}_{\mathbf{xr}}(\hat{\alpha}_1(t_i), \hat{\alpha}_2(t_i), \dots, \hat{\alpha}_D(t_i))^H \hat{\mathbf{R}}_{\mathbf{xx}}^{-1}(t_i) \\
 \hat{\mathbf{r}}_{\mathbf{xr}}(\hat{\alpha}_1(t_i), \hat{\alpha}_2(t_i), \dots, \hat{\alpha}_D(t_i)) &\approx \sum_{d=0}^D \left\{ \sum_{u=1}^D \sum_{v=1}^D \frac{1}{i^2} \sum_{l=0}^{i-1} \sum_{k=0}^{i-1} \left\{ s_d(l) s_d(l) \right. \right. \\
 & e^{-j2\pi l \hat{\alpha}_u T_s} \left. \right\}^* \times \left\{ s_d(k) s_d(k) e^{-j2\pi k \hat{\alpha}_v T_s} \right\} \left. \right\} \times \left\{ \mathbf{a}(\theta_d)^H \hat{\mathbf{R}}_{\mathbf{xx}}^{-1}(t_i) \mathbf{a}(\theta_d) \right\} \\
 & \times \left\{ \mathbf{c}^H \mathbf{a}^*(\theta_d) \mathbf{a}^T(\theta_d) \mathbf{c} \right\} + \sum_{j=D+1}^{D+J} \left\{ \sum_{u=1}^D \sum_{v=1}^D \frac{1}{i^2} \sum_{l=0}^{i-1} \sum_{k=0}^{i-1} \left\{ s_j(l) s_j(l) e^{-j2\pi l \hat{\alpha}_u T_s} \right\}^* \right. \\
 & \left. \times \left\{ s_j(k) s_j(k) e^{-j2\pi k \hat{\alpha}_v T_s} \right\} \right\} \times \left\{ \mathbf{a}(\theta_j)^H \hat{\mathbf{R}}_{\mathbf{xx}}^{-1}(t_i) \mathbf{a}(\theta_j) \right\} \times \left\{ \mathbf{c}^H \mathbf{a}^*(\theta_j) \mathbf{a}^T(\theta_j) \mathbf{c} \right\} \\
 & = \sum_{d=1}^D \left[ \left\{ \sum_{u=1}^D \sum_{v=1}^D \hat{R}_{s_d s_d^*}(\hat{\alpha}_u, 0)^* \hat{R}_{s_d s_d^*}(\hat{\alpha}_v, 0) \right\} \times \left\{ \mathbf{a}(\theta_d)^H \hat{\mathbf{R}}_{\mathbf{xx}}^{-1}(t_i) \mathbf{a}(\theta_d) \right\} \right. \\
 & \left. \times \left\{ \mathbf{c}^H \mathbf{a}^*(\theta_d) \mathbf{a}^T(\theta_d) \mathbf{c} \right\} \right] + \sum_{j=D+1}^{D+J} \left[ \left\{ \sum_{u=1}^D \sum_{v=1}^D \hat{R}_{s_j s_j^*}(\hat{\alpha}_u, 0)^* \hat{R}_{s_j s_j^*}(\hat{\alpha}_v, 0) \right\} \right. \\
 & \left. \times \left\{ \mathbf{a}(\theta_j)^H \hat{\mathbf{R}}_{\mathbf{xx}}^{-1}(t_i) \mathbf{a}(\theta_j) \right\} \times \left\{ \mathbf{c}^H \mathbf{a}^*(\theta_j) \mathbf{a}^T(\theta_j) \mathbf{c} \right\} \right]. \tag{30}
 \end{aligned}$$

The cross terms disappear in (30) because of the stationarity of  $\mathbf{n}(t)$  and the assumed uncorrelation among  $s_d(t)$ ,  $s_j(t)$ , and  $\mathbf{n}(t)$ . From (30), we can rewrite (21) as

$$\begin{aligned}
\nabla_{\hat{\alpha}_d} Q(\hat{\alpha}_1(t_i), \hat{\alpha}_2(t_i), \dots, \hat{\alpha}_D(t_i)) &= \frac{\partial Q(\hat{\alpha}_1(t_i), \hat{\alpha}_2(t_i), \dots, \hat{\alpha}_D(t_i))}{\partial \hat{\alpha}_d} \\
&\approx \sum_{d=1}^D \left[ \left[ \partial \left\{ \sum_{u=1}^D \sum_{v=1}^D \hat{R}_{s_d s_d^*}(\hat{\alpha}_u, 0)^* \hat{R}_{s_d s_d^*}(\hat{\alpha}_v, 0) \right\} / \partial \hat{\alpha}_d \right] \right. \\
&\quad \times \left. \left\{ \mathbf{a}(\theta_d)^H \hat{\mathbf{R}}_{\mathbf{xx}}^{-1}(t_i) \mathbf{a}(\theta_d) \right\} \times \left\{ \mathbf{c}^H \mathbf{a}^*(\theta_d) \mathbf{a}^T(\theta_d) \mathbf{c} \right\} \right] \\
&\quad + \sum_{j=1}^J \left[ \left[ \partial \left\{ \sum_{u=1}^D \sum_{v=1}^D \hat{R}_{s_j s_j^*}(\hat{\alpha}_u, 0)^* \hat{R}_{s_j s_j^*}(\hat{\alpha}_v, 0) \right\} / \partial \hat{\alpha}_d \right] \right. \\
&\quad \times \left. \left\{ \mathbf{a}(\theta_j)^H \hat{\mathbf{R}}_{\mathbf{xx}}^{-1}(t_i) \mathbf{a}(\theta_j) \right\} \times \left\{ \mathbf{c}^H \mathbf{a}^*(\theta_j) \mathbf{a}^T(\theta_j) \mathbf{c} \right\} \right]. \tag{31}
\end{aligned}$$

Consider BPSK signals. We set

$$s_d(t) = A_d e^{j(\pi \alpha_d t + \Phi_{s_d}(t))} \quad \text{and} \quad s_j(t) = A_j e^{j(\pi \alpha_j t + \Phi_{s_j}(t))}, \tag{32}$$

where  $A_d$  and  $A_j$  are the constant amplitudes, and  $\Phi_{s_d}(t)$  and  $\Phi_{s_j}(t)$  are the random phases equal to  $\pm(\pi/2)$  for  $d = 1, 2, \dots, D$  and  $j = D + 1, \dots, D + J$ , respectively. Accordingly, we have

$$\begin{aligned}
\hat{R}_{s_d s_d^*}(\hat{\alpha}_u, 0) &= -A_d^2 \text{sinc}((\hat{\alpha}_u - \alpha_d)T) \\
\text{and } \hat{R}_{s_j s_j^*}(\hat{\alpha}_u, 0) &= -A_j^2 \text{sinc}((\hat{\alpha}_u - \alpha_j)T). \tag{33}
\end{aligned}$$

Based on (32), it can be shown that

$$\begin{aligned}
&\partial \left\{ \sum_{u=1}^D \sum_{v=1}^D \hat{R}_{s_d s_d^*}(\hat{\alpha}_u, 0)^* \hat{R}_{s_d s_d^*}(\hat{\alpha}_v, 0) \right\} / \partial \hat{\alpha}_d \\
&= A_d^4 \left\{ \begin{aligned} &\sum_{v=1}^D \frac{\partial \text{sinc}((\hat{\alpha}_d - \alpha_d)T)}{\partial \hat{\alpha}_d} \text{sinc}((\hat{\alpha}_v - \alpha_d)T) + \\ &\sum_{u=1}^D \frac{\partial \text{sinc}((\hat{\alpha}_d - \alpha_d)T)}{\partial \hat{\alpha}_d} \text{sinc}((\hat{\alpha}_u - \alpha_d)T) \end{aligned} \right\}
\end{aligned}$$

and

$$\begin{aligned} & \partial \left\{ \sum_{u=1}^D \sum_{v=1}^D \hat{R}_{s_j s_j^*}(\hat{\alpha}_u, 0)^* \hat{R}_{s_j s_j^*}(\hat{\alpha}_v, 0) \right\} / \partial \hat{\alpha}_d \\ &= A_d^4 \left\{ \begin{aligned} & \sum_{v=1}^D \frac{\partial \text{sinc}((\hat{\alpha}_d - \alpha_j)T)}{\partial \hat{\alpha}_d} \text{sinc}((\hat{\alpha}_v - \alpha_j)T) + \\ & \sum_{u=1}^D \frac{\partial \text{sinc}((\hat{\alpha}_d - \alpha_j)T)}{\partial \hat{\alpha}_d} \text{sinc}((\hat{\alpha}_u - \alpha_j)T) \end{aligned} \right\}. \quad (34) \end{aligned}$$

Let  $\hat{\alpha}_d = \alpha_d + \Delta\alpha_d$  and  $\hat{\alpha}_d - \alpha_q = \Delta\alpha_{dq}$ . It is appropriate to consider the case where the interval  $T = iT_s$  is so large that all the terms  $\text{sinc}(\Delta\alpha_{dq}T)$  are negligible for all  $d \neq q$ . Therefore, we can approximate (34) as follows:

$$\begin{aligned} & \partial \left\{ \sum_{u=1}^D \sum_{v=1}^D \hat{R}_{s_d s_d^*}(\hat{\alpha}_u, 0)^* \hat{R}_{s_d s_d^*}(\hat{\alpha}_v, 0) \right\} / \partial \hat{\alpha}_d |_{\hat{\alpha}_d = \hat{\alpha}_d(i)} \\ &= 2A_d^4 \frac{\partial \text{sinc}(\Delta\alpha_d iT_s)}{\partial \Delta\alpha_d} |_{\Delta\alpha_d = \Delta\alpha_d(i)} \text{sinc}(\Delta\alpha_d(i) iT_s) \\ &= 2 \frac{\pi \Delta\alpha_d(i) iT_s \cos(\pi \Delta\alpha_d(i) iT_s) - \sin(\pi \Delta\alpha_d(i) iT_s)}{\pi \Delta\alpha_d^2(i) iT_s} A_d^4 \text{sinc}(\Delta\alpha_d(i) iT_s) \end{aligned}$$

and  $\partial \left\{ \sum_{u=1}^D \sum_{v=1}^D \hat{R}_{s_j s_j^*}(\hat{\alpha}_u, 0)^* \hat{R}_{s_j s_j^*}(\hat{\alpha}_v, 0) \right\} / \partial \hat{\alpha}_d \approx 0$  (35)

if we can make sure that the following condition given by

$$|\Delta\alpha_d(i) \{iT_s\}| \leq \frac{1}{2} \quad (36)$$

is satisfied, where  $\Delta\alpha_d(i) = \hat{\alpha}_d(i) - \alpha_d$  denotes the estimation error of  $\alpha_d$  at the time instant  $T = iT_s$ . As a result, (31) becomes

$$\begin{aligned} \nabla_{\hat{\alpha}_d} Q(\hat{\alpha}_1(t_i), \hat{\alpha}_2(t_i), \dots, \hat{\alpha}_D(t_i)) &= \frac{\partial Q(\hat{\alpha}_1(t_i), \hat{\alpha}_2(t_i), \dots, \hat{\alpha}_D(t_i))}{\partial \hat{\alpha}_d} \\ &\approx \sum_{d=1}^D \left[ \left[ 2 \frac{\pi \Delta\alpha_d(i) iT_s \cos(\pi \Delta\alpha_d(i) iT_s) - \sin(\pi \Delta\alpha_d(i) iT_s)}{\pi \Delta\alpha_d^2(i) iT_s} A_d^4 \right. \right. \\ & \left. \left. \text{sinc}(\Delta\alpha_d(i) iT_s) \right] \times \left\{ \mathbf{a}(\theta_d)^H \hat{\mathbf{R}}_{\mathbf{xx}}^{-1}(t_i) \mathbf{a}(\theta_d) \right\} \times \left\{ \mathbf{c}^H \mathbf{a}^*(\theta_d) \mathbf{a}^T(\theta_d) \mathbf{c} \right\} \right] \quad (37) \end{aligned}$$

and the term  $\langle \mathbf{x}(t)\mathbf{x}^T(t)e^{-j2\pi\hat{\alpha}_d(t_i)t(-j2\pi t)} \rangle_{t_i}$  of (24) becomes

$$\begin{aligned} \langle \mathbf{x}(t)\mathbf{x}^T(t)e^{-j2\pi\hat{\alpha}_d(t_i)t(-j2\pi t)} \rangle_{t_i} &\approx \sum_{d=1}^D \frac{A_d^2 e^{-j\pi\Delta\alpha_d(i)iT_s}}{\pi\Delta\alpha_d^2(i)iT_s} \\ &\times \left\{ \begin{aligned} &\sin(\pi\Delta\alpha_d(i)iT_s) - \pi\Delta\alpha_d(i)iT_s \cos(\pi\Delta\alpha_d(i)iT_s) \\ &+ j\pi\Delta\alpha_d(i)iT_s \sin(\pi\Delta\alpha_d(i)iT_s) \end{aligned} \right\} \mathbf{a}(\theta_d)\mathbf{a}(\theta_d)^T. \end{aligned} \quad (38)$$

We note that the maximum singular value of (38) is approximately equal to

$$\frac{M^2 A_d^2}{\pi\Delta\alpha_d^2(i)iT_s} \left| \begin{aligned} &\sin(\pi\Delta\alpha_d(i)iT_s) - \pi\Delta\alpha_d(i)iT_s \cos(\pi\Delta\alpha_d(i)iT_s) \\ &+ j\pi\Delta\alpha_d(i)iT_s \sin(\pi\Delta\alpha_d(i)iT_s) \end{aligned} \right|. \quad (39)$$

Therefore, the step-size parameter of (24) is approximately given by

$$\begin{aligned} \nu_d(t_i) &= \frac{1}{\left\| \langle \mathbf{x}(t)\mathbf{x}^T(t)e^{-j2\pi\hat{\alpha}_d(t_i)t(-j2\pi t)} \rangle_{t_i} \right\|^{p_d}} \\ &\approx \left\{ \frac{M^2 A_d^2}{\pi\Delta\alpha_d^2(i)iT_s} \left| \begin{aligned} &\sin(\pi\Delta\alpha_d(i)iT_s) - \pi\Delta\alpha_d(i)iT_s \cos(\pi\Delta\alpha_d(i)iT_s) \\ &+ j\pi\Delta\alpha_d(i)iT_s \sin(\pi\Delta\alpha_d(i)iT_s) \end{aligned} \right| \right\}^{-p_d}. \end{aligned} \quad (40)$$

Next, we consider the objective function shown by (30). After substituting (33) into (30), we have

$$\begin{aligned} Q(\hat{\alpha}_1(t_i), \hat{\alpha}_2(t_i), \dots, \hat{\alpha}_D(t_i)) &= \hat{\mathbf{r}}_{\mathbf{x}r}(\hat{\alpha}_1(t_i), \hat{\alpha}_2(t_i), \dots, \hat{\alpha}_D(t_i))^H \hat{\mathbf{R}}_{\mathbf{xx}}^{-1}(t_i) \\ \hat{\mathbf{r}}_{\mathbf{x}r}(\hat{\alpha}_1(t_i), \hat{\alpha}_2(t_i), \dots, \hat{\alpha}_D(t_i)) &= \sum_{d=1}^D \left[ \left\{ \sum_{u=1}^D \sum_{v=1}^D A_d^4 \text{sinc}((\hat{\alpha}_u - \alpha_d)T) \right. \right. \\ &\text{sinc}((\hat{\alpha}_v - \alpha_d)T) \left. \left. \right\} \times \left\{ \mathbf{a}(\theta_d)^H \hat{\mathbf{R}}_{\mathbf{xx}}^{-1}(t_i) \mathbf{a}(\theta_d) \right\} \times \left\{ \mathbf{c}^H \mathbf{a}^*(\theta_d) \mathbf{a}^T(\theta_d) \mathbf{c} \right\} \right] \\ &+ \sum_{j=D+1}^{D+J} \left[ \left\{ \sum_{u=1}^D \sum_{v=1}^D A_j^4 \text{sinc}((\hat{\alpha}_u - \alpha_j)T) \text{sinc}((\hat{\alpha}_v - \alpha_j)T) \right\} \right. \\ &\times \left. \left\{ \mathbf{a}(\theta_j)^H \hat{\mathbf{R}}_{\mathbf{xx}}^{-1}(t_i) \mathbf{a}(\theta_j) \right\} \times \left\{ \mathbf{c}^H \mathbf{a}^*(\theta_j) \mathbf{a}^T(\theta_j) \mathbf{c} \right\} \right]. \end{aligned} \quad (41)$$

Again, we can approximate (41) as follows:

$$\begin{aligned} Q(\hat{\alpha}_1(t_i), \hat{\alpha}_2(t_i), \dots, \hat{\alpha}_D(t_i)) &= \hat{\mathbf{r}}_{\mathbf{x}r}(\hat{\alpha}_1(t_i), \hat{\alpha}_2(t_i), \dots, \hat{\alpha}_D(t_i))^H \hat{\mathbf{R}}_{\mathbf{xx}}^{-1}(t_i) \\ \hat{\mathbf{r}}_{\mathbf{x}r}(\hat{\alpha}_1(t_i), \hat{\alpha}_2(t_i), \dots, \hat{\alpha}_D(t_i)) &\approx \sum_{d=1}^D \left\{ A_d^4 \text{sinc}^2(\Delta\alpha_d T) \right\} \times \left\{ \mathbf{a}(\theta_d)^H \right. \\ &\hat{\mathbf{R}}_{\mathbf{xx}}^{-1}(t_i) \mathbf{a}(\theta_d) \left. \right\} \times \left\{ \mathbf{c}^H \mathbf{a}^*(\theta_d) \mathbf{a}^T(\theta_d) \mathbf{c} \right\} \end{aligned} \quad (42)$$

when the interval  $T = iT_s$  is so large that all the terms  $\text{sinc}(\Delta\alpha_d T)$  are negligible for all  $d \neq q$ .

From the update formula of (23), we have that

$$\begin{aligned} \Delta\alpha_d(t_{i+1}) &= \Delta\alpha_d(t_i) + \nu_d(t_i) \nabla_{\hat{\alpha}_d} Q(\hat{\alpha}_1, \hat{\alpha}_2, \dots, \hat{\alpha}_D) \\ \hat{\alpha}_1 &= \hat{\alpha}_1(t_i), \hat{\alpha}_2 = \hat{\alpha}_2(t_i), \dots, \hat{\alpha}_D = \hat{\alpha}_D(t_i) \end{aligned} \quad (43)$$

and

$$\begin{aligned} \Delta\alpha_d(i+1)(i+1)T_s &\approx \\ &\left\{ \begin{aligned} &\Delta\alpha_d(i) + 2M^{-2p_d} A_s^{4-2p_d} \left\{ \mathbf{a}(\theta_d)^H \hat{\mathbf{R}}_{\mathbf{xx}}^{-1}(t_i) \mathbf{a}(\theta_d) \right\} \\ &\times \left\{ \mathbf{c}^H \mathbf{a}(\theta_d)^* \mathbf{a}(\theta_d)^T \mathbf{c} \right\} \\ &\times \text{sinc}(\Delta\alpha_d(i)iT_s) \\ &\times \frac{\pi \Delta\alpha_d(i)iT_s \cos(\pi \Delta\alpha_d(i)iT_s) - \sin(\pi \Delta\alpha_d(i)iT_s)}{(\pi \Delta\alpha_d^2(i)iT_s)^{1-p_d}} \\ &\times |\sin(\pi \Delta\alpha_d(i)iT_s) - \pi \Delta\alpha_d(i)iT_s \cos(\pi \Delta\alpha_d(i)iT_s) \\ &+ j\pi \Delta\alpha_d(i)iT_s \sin(\pi \Delta\alpha_d(i)iT_s)|^{-p_d} \end{aligned} \right\} (i+1)T_s. \end{aligned} \quad (44)$$

Setting  $\Delta\alpha_d(i)(iT_s)$  to the extreme value 1/2 and performing some necessary algebraic manipulations, we have the following approximation

$$\Delta\alpha_d(i+1)(i+1)T_s \approx \frac{1}{2} + \frac{1}{2i} - \Omega \times \frac{i+1}{i^{p_d-1}}, \quad (45)$$

where  $\Omega = \left\{ \begin{aligned} &2^{4-2p_d} \pi^{p_d-2} M^{-2p_d} A_s^{4-2p_d} \left\{ \mathbf{a}(\theta_d)^H \hat{\mathbf{R}}_{\mathbf{xx}}^{-1}(t_i) \mathbf{a}(\theta_d) \right\} \\ &\times \left\{ \mathbf{c}^H \mathbf{a}(\theta_d)^* \mathbf{a}(\theta_d)^T \mathbf{c} \right\} T_s^{2-p_d} \end{aligned} \right\} \times \left(1 + \frac{\pi^2}{4}\right)^{-p_d/2}$ .  $\Omega$  is always non-negative and approximately independent of  $i$  by neglecting the finite sample effect. Under the condition  $|\Delta\alpha_d(i)\{iT_s\}| \leq \frac{1}{2}$  of (36), we have that

$$-1 \leq \frac{1}{2(i-1)} - \Omega \frac{i}{(i-1)^{p_d-1}} \leq 0. \quad (46)$$

Equation (46) leads to that

$$\frac{(i-1)^{p_d-2}}{2i} \leq \Omega \leq \frac{(2i-1)(i-1)^{p_d-2}}{2i}. \quad (47)$$

Based on (36), we have to ensure that  $|\Delta\alpha_d(i+1)(i+1)T_s| \leq \frac{1}{2}$ . From (47), we obtain

$$\frac{1}{2i} - \frac{(2i-1)(i+1)}{2i^{p_d}(i-1)^{2-p_d}} \leq \frac{1}{2i} - \Omega \frac{i+1}{i^{p_d-1}} \leq \frac{1}{2i} - \frac{i+1}{2i^{p_d}(i-1)^{2-p_d}}. \quad (48)$$

Hence, setting  $1 \leq p_d \leq 2$  leads to

$$\frac{1}{2i} - \frac{i+1}{2i^{p_d}(i-1)^{2-p_d}} = \frac{1}{2i} \left[ 1 - \left( \frac{i+1}{i} \right)^{p_d-1} \left( \frac{i+1}{i-1} \right)^{2-p_d} \right] \leq 0$$

and  $\frac{1}{2i} - \frac{(2i-1)(i+1)}{2i^{p_d}(i-1)^{2-p_d}} > -1$  if  $p_d = 2$  and  $< -1$  if  $p_d = 1$ . Therefore, there exists some  $p_d$  between 1 and 2 such that  $|\Delta\alpha_d(i+1)(i+1)T_s| \leq \frac{1}{2}$  for  $d = 1, 2, \dots, D$ . Following the similar procedure, we can prove that the conclusion is also valid for substituting the other extreme value  $-1/2$  for  $\Delta\alpha_d(i)(iT_s)$  into (44) and performing some necessary algebraic manipulations.

## 6. COMPUTER SIMULATION EXAMPLES

Here, we present several simulation examples for showing the effectiveness of the proposed approach. For all simulation examples, the inter-element spacing =  $\lambda/2$ , where  $\lambda$  is the wavelength of the BPSK SOIs with rectangular pulse shape and baud rate =  $5/11$ . The interferers are also rectangular pulse shaped BPSK signals with baud rate =  $5/11$ . The noise received by the arrays is spatially white. The sampling interval for obtaining data snapshots is set to 0.1. The vector  $\mathbf{c}$  for the original LS-SCORE algorithm and the proposed approach is fixed to  $\mathbf{c} = [1, 0, 0, \dots, 0]^T$ . The time delay  $\tau$  is set to 0. All the simulation results are obtained by averaging 50 independent runs. The first received 110 data snapshots are used for computing all the initial sample correlation matrices. The values of the parameters  $q_d$  used by the robust approach of [9] and the parameters  $p_d$  used by the proposed approach for  $d = 1, 2, \dots, D$  are appropriately determined by experiment. The SINR at the array output is computed as follows:

$$\text{SINR} = \frac{\hat{\mathbf{w}}_{\text{new}}^H \hat{\mathbf{R}}_{\text{ss}} \hat{\mathbf{w}}_{\text{new}}}{\hat{\mathbf{w}}_{\text{new}}^H \hat{\mathbf{R}}_{\text{ii}} \hat{\mathbf{w}}_{\text{new}}}, \quad (49)$$

where  $\hat{\mathbf{R}}_{\text{ss}}$  and  $\hat{\mathbf{R}}_{\text{ii}}$  are the sample versions of  $\mathbf{R}_{\text{ss}}$  and  $\mathbf{R}_{\text{ii}}$ , respectively.  $\mathbf{R}_{\text{ss}}$  and  $\mathbf{R}_{\text{ii}}$  are computed according to (14) and (15), respectively.  $\hat{\mathbf{w}}_{\text{new}}$  is computed by (16).

*Example 1:* We use a uniform linear array (ULA) with  $M = 12$  and multiple SOIs. Two SOIs have cycle frequencies  $\alpha_1 = 2$  and  $\alpha_2 = 2.8$ , direction angles  $\theta_1 = 5^\circ$  and  $\theta_2 = 60^\circ$ , and signal-to-noise ratio (SNR) equal to 2 dB and 3 dB, respectively, while two interferers have cycle frequencies  $\alpha_3 = 4.6$  and  $\alpha_4 = 7.8$ , direction angles  $\theta_3 = 30^\circ$  and  $\theta_4 = 40^\circ$ , and interference-to-noise ratio (INR) equal to 10 dB. The CFEs for the two SOIs are set to  $\Delta\alpha_1 =$

0.02 and  $\Delta\alpha_2 = -0.02$ . Figure 1 plots the array beam patterns with 2530 data snapshots obtained by using the original LS-SCORE algorithm [3] with and without CFE, the robust approach of [9] with the parameters  $q_1 = q_2 = 1.5$ , and the proposed approach with and without CFE, respectively. The parameters  $p_1$  and  $p_2$  are set to 1.32 and 1.3, respectively for the proposed approach. The array output SINRs are  $-12.776$ ,  $10.532$ ,  $7.949$ ,  $12.736$ , and  $12.949$  dB, respectively. Figure 2 depicts the array output SINR versus the number of data snapshots. Figure 3 demonstrates the array output SINR versus the CFE. The CFE sequences of  $\Delta\alpha_1$  and  $\Delta\alpha_2$  are  $[0.01, 0.02, \dots, 0.06]$  and  $[-0.01, -0.02, \dots, -0.06]$ , respectively. We note that the proposed approach is effective in dealing with the CFE problem and provides the performance better than that of using the original LS-SCORE algorithm without CFE.

*Example 2:* We use a ULA with  $M = 18$  and multiple SOIs. Three SOIs have cycle frequencies  $\alpha_1 = 2$ ,  $\alpha_2 = 2.8$ , and  $\alpha_3 = 9.4$ , direction angles  $\theta_1 = -15^\circ$ ,  $\theta_2 = 15^\circ$ , and  $\theta_3 = 75^\circ$ , and SNR equal to 5 dB, while two interferers have cycle frequencies  $\alpha_3 = 4.6$  and  $\alpha_4 = 7.8$ , direction angles  $\theta_3 = 40^\circ$  and  $\theta_4 = 50^\circ$ , and INR equal to 15 dB. The CFEs for the SOIs are set to  $\Delta\alpha_1 = \Delta\alpha_2 = \Delta\alpha_3 = 0.02$ . Figure 4 plots the array beam patterns with 2530 data snapshots obtained by using the original LS-SCORE algorithm [3] with and without CFE, the robust approach of [9] with the parameters  $q_1 = q_2 = q_3 = 1.8$ , and the proposed approach with and without CFE, respectively. The parameters  $p_1$ ,  $p_2$ , and  $p_3$  are all set to 1.32 for the proposed approach. The array output SINRs are  $-16.236$ ,  $8.625$ ,  $3.141$ ,  $16.957$ , and  $17.057$  dB, respectively. Figure 5 depicts the array output SINR versus the number of data snapshots. Figure 6 shows the array output SINR

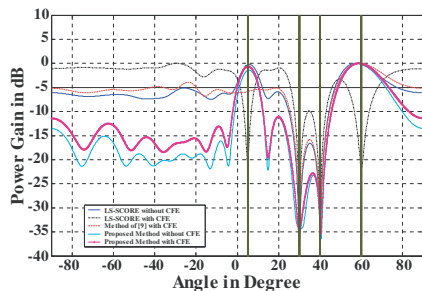


**Figure 1.** The array beam patterns for *Example 1*.

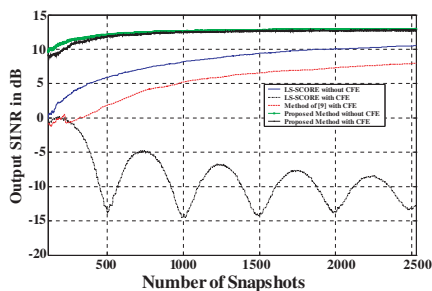


**Figure 2.** The array output SINR versus the number of data snapshots for *Example 1*.

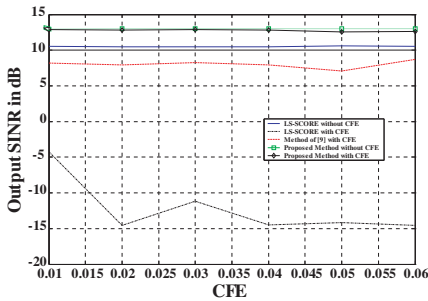


**Figure 3.** The array output SINR versus CFE for *Example 1*.

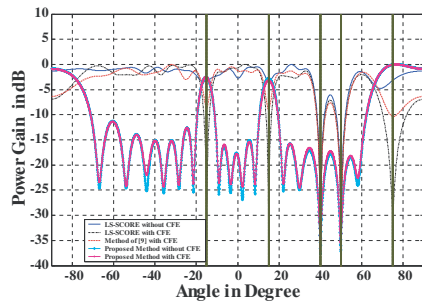


**Figure 4.** The array beam patterns for *Example 2*.

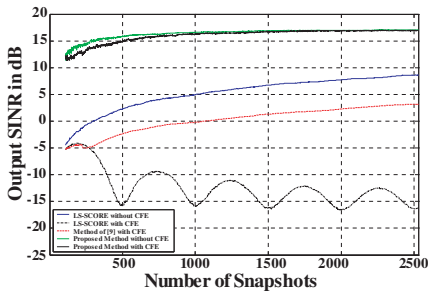


**Figure 5.** The array output SINR versus the number of data snapshots for *Example 2*.

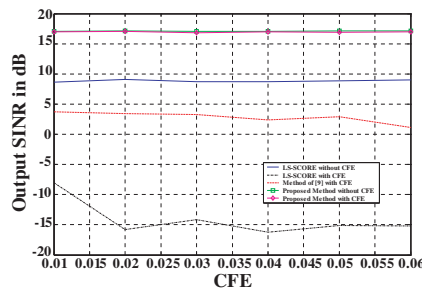


**Figure 6.** The array output SINR versus CFE for *Example 2*.

versus the CFE. The CFE sequences of  $\Delta\alpha_1$ ,  $\Delta\alpha_2$ , and  $\Delta\alpha_3$  are all set to  $[0.01, 0.02, \dots, 0.06]$ . Again, we note that the proposed approach is effective in dealing with the CFE in this case.

*Example 3:* We use a two-dimensional (2-D) uniform circular array (UCA) with  $M = 12$  and multiple SOIs. Two SOIs have cycle frequencies  $\alpha_1 = 2$  and  $\alpha_2 = 2.8$ , elevation angles  $\theta_1 = 10^\circ$  and  $\theta_2 = 55^\circ$ , azimuth angles  $\phi_1 = 20^\circ$  and  $\phi_2 = 90^\circ$ , and SNRs equal to 5 dB, respectively, while two interferers have cycle frequencies  $\alpha_3 = 4.6$  and  $\alpha_4 = 7.8$ , elevation angles  $\theta_3 = 35^\circ$  and  $\theta_4 = 80^\circ$ , azimuth angles  $\phi_3 = 80^\circ$  and  $\phi_4 = 70^\circ$ , and INR equal to 10 dB. The CFEs for the two SOIs are set to  $\Delta\alpha_1 = 0.02$  and  $\Delta\alpha_2 = -0.02$ . Figure 7 depicts the array output SINR versus the number of data snapshots obtained by using the original LS-SCORE algorithm [3] with and without CFE, the robust approach of [9] with the parameters  $q_1 = q_2 = 1.5$ , and the proposed approach with and without CFE, respectively. Both of the parameters  $p_1$  and  $p_2$  are set to 1.3 for the proposed approach.

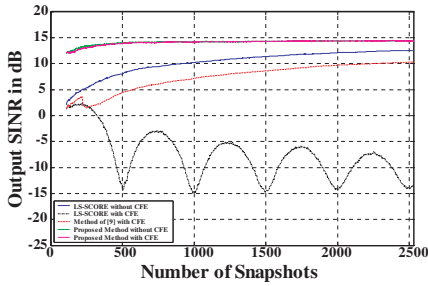


**Figure 7.** The array output SINR versus the number of data snapshots for *Example 3*.

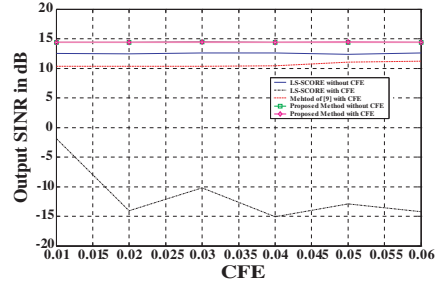


**Figure 8.** The array output SINR versus CFE for *Example 3*.

The array output SINRs obtained at the number of snapshots equal to 2530 are  $-13.424$ ,  $12.540$ ,  $10.274$ ,  $14.368$ , and  $14.385$  dB, respectively. Figure 8 shows the array output SINR versus the CFE. The CFE sequences of  $\Delta\alpha_1$  and  $\Delta\alpha_2$  are  $[0.01, 0.02, \dots, 0.06]$  and  $[-0.01, -0.02, \dots, -0.06]$ , respectively. We note that the proposed approach works well in dealing with the 2-D UCA blind beamforming under the CFE.

As to the selection of the parameters  $p_1$ ,  $p_2$ , and  $p_3$ , they are determined according to the convergence constraint presented in Section 5 and the beamforming performance of the antenna array. According to our experience, the parameters  $p_1$ ,  $p_2$ , and  $p_3$  are first set to 1.5 to satisfy the convergence constraint  $1 \leq p_d \leq 2$ ,  $d = 1, 2, 3$ . Then, we adjust the parameters  $p_1$ ,  $p_2$ , and  $p_3$  by adding 0.02 to or subtracting 0.02 from 1.5. This procedure continues until a satisfactory beamforming performance is obtained.

## 7. CONCLUSION

This paper has presented an approach for blind adaptive array beamforming in the presence of cycle frequency error (CFE). Based on the exploitation of signal cyclostationarity and diagonal loading, we have developed a cyclic sample matrix inversion (C-SMI) beamformer for simultaneously extracting multiple desired signals with distinct cycle frequencies. The C-SMI beamformer shows the capability against the effects of cycle leakage due to finite data samples. An iterative algorithm with the exploitation of signal cyclostationarity for optimizing a novel objective function has been presented to make the C-SMI beamformer robust against CFE. The convergence property regarding the iterative algorithm has been investigated. Simulation results have confirmed the effectiveness of the theoretical work. A

further research work on the extension of the proposed approach to deal with random cycle frequency mismatch as discussed in [15] is currently under investigation.

## APPENDIX A.

From (7) and (8), the cross-correlation vector of  $\mathbf{x}(t)$  and  $r(t)$  is computed over  $[0, T]$  as follows:

$$\begin{aligned} \hat{\mathbf{r}}_{\mathbf{x}r}(\alpha_1, \alpha_2, \dots, \alpha_D) &= \left\langle \mathbf{x}(t)r^*(t) \right\rangle_T \\ &= \left\langle \left( \sum_{d=1}^D s_d(t)\mathbf{a}(\theta_d) + \mathbf{i}(t) \right) \left( \sum_{d=1}^D e^{j2\pi\alpha_d t} \mathbf{c}^H \mathbf{x}^*(t-\tau) \right)^* \right\rangle_T. \end{aligned} \quad (\text{A1})$$

As  $T$  approaches infinity, it follows from the proof of [7] that (A1) can be approximated by

$$\begin{aligned} \lim_{T \rightarrow \infty} \hat{\mathbf{r}}_{\mathbf{x}r}(\alpha_1, \alpha_2, \dots, \alpha_D) &= \lim_{T \rightarrow \infty} \langle \mathbf{x}(t)r^*(t) \rangle_T = \mathbf{r}_{\mathbf{x}r}(\alpha_1, \alpha_2, \dots, \alpha_D) \\ &= \langle \mathbf{x}(t)r^*(t) \rangle_{\infty} = \sum_{d=1}^D k_d R_{s_d s_d^*}(\alpha_d, \tau) \mathbf{a}(\theta_d) = \sum_{d=1}^D S_d \mathbf{a}(\theta_d), \end{aligned} \quad (\text{A2})$$

where  $k_d = \mathbf{a}^T(\theta_d) \mathbf{c} e^{-j\pi\alpha_d \tau}$ ,  $R_{s_d s_d^*}(\alpha_d, \tau) = \langle s_d(t)s_d(t-\tau)e^{-j2\pi\alpha_d t} \rangle_{\infty}$ , and  $S_d = k_d R_{s_d s_d^*}(\alpha_d, \tau)$ . From (A2), we note that the parameter  $S_d$ , for  $d = 1, 2, \dots, D$ , can be obtained as follows. From (2), the CCM  $\mathbf{R}_{\mathbf{x}\mathbf{x}}(\alpha_d, \tau)$  is given by

$$\mathbf{R}_{\mathbf{x}\mathbf{x}}(\alpha_d, \tau) = \langle \mathbf{x}(t)\mathbf{x}^H(t-\tau)e^{-j2\pi\alpha_d t} \rangle_{\infty} = R_{s_d s_d}(\alpha_d, \tau) \mathbf{a}(\theta_d) \mathbf{a}^H(\theta_d). \quad (\text{A3})$$

Hence, we have

$$\text{trace}\{\mathbf{R}_{\mathbf{x}\mathbf{x}}(\alpha_d, \tau)\} = R_{s_d s_d}(\alpha_d, \tau) \mathbf{a}^H(\theta_d) \mathbf{a}(\theta_d) = M R_{s_d s_d}(\alpha_d, \tau). \quad (\text{A4})$$

Accordingly, the CCF  $R_{s_d s_d}(\alpha_d, \tau)$  of  $s_d(t)$  can be obtained from (A4) as follows:  $R_{s_d s_d}(\alpha_d, \tau) = \text{trace}\{\mathbf{R}_{\mathbf{x}\mathbf{x}}(\alpha_d, \tau)\}/M$ . Next, setting the  $M \times 1$  control vector to  $\mathbf{c} = [100 \dots 0]^T$  and  $\tau = 0$ , we have  $k_d = \mathbf{a}^T(\theta_d) \mathbf{c} e^{-j\pi\tau} = 1$  since the first array sensor is the reference. As a result,  $S_d$  is given by

$$S_d = R_{s_d s_d^*}(\alpha_d, 0) = \{\rho_{s_d s_d^*}(\alpha_d, 0) \text{trace}\{\mathbf{R}_{\mathbf{x}\mathbf{x}}(\alpha_d, 0)\}\} / \{M \rho_{s_d s_d}(\alpha_d, 0)\}, \quad (\text{A5})$$

for  $d = 1, 2, \dots, D$ . It follows that (A2) can be rewritten as

$$\begin{aligned} \mathbf{r}_{\mathbf{x}r}(\alpha_1, \alpha_2, \dots, \alpha_D) &= \lim_{T \rightarrow \infty} \hat{\mathbf{r}}_{\mathbf{x}r}(\alpha_1, \alpha_2, \dots, \alpha_D) = \lim_{T \rightarrow \infty} \langle \mathbf{x}(t)r^*(t) \rangle_T \\ &= \sum_{d=1}^D S_d \mathbf{a}(\theta_d) = \sum_{d=1}^D \{\rho_{s_d s_d^*}(\alpha_d, 0) \text{trace}\{\mathbf{R}_{\mathbf{x}\mathbf{x}}(\alpha_d, 0)\}\} \mathbf{a}(\theta_d) / \{M \rho_{s_d s_d}(\alpha_d, 0)\}. \end{aligned} \quad (\text{A6})$$

## ACKNOWLEDGMENT

This work was supported by the National Science Council of TAIWAN under Grants NSC96-2221-E002-086 and NSC97-2221-E002-174-MY3. The author would like to thank Mr. H.-H. Chan for his help in preparing MATLAB programs to obtain the simulation results presented in the paper.

## REFERENCES

1. Monzingo, R. A. and T. W. Miller, *Introduction to Adaptive Arrays*, John Wiley, New York, 1980.
2. Compton, Jr., R. T., *Adaptive Antennas, Concepts, and Performance*, Prentice Hall, Englewood Cliffs, NJ, 1989.
3. Agee, B. G., S. V. Schell, and W. A. Gardner, "Spectral self-coherence restoral: A new approach to blind adaptive signal extraction using antenna arrays," *Proc. IEEE*, Vol. 78, No. 4, 753-767, Apr. 1990.
4. Gardner, W. A., "Spectral correlation of modulated signals: Part I — Analog modulation," *IEEE Trans. on Commun.*, Vol. 35, No. 6, 584-594, Jun. 1987.
5. Gardner, W., W. Brown, and C.-K. Chen, "Spectral correlation of modulated signals: Part II — Digital modulation," *IEEE Trans. on Commun.*, Vol. 35, No. 6, 595-601, Jun. 1987.
6. Wu, Q. and K. M. Wong, "Blind adaptive beamforming for cyclostationary signals," *IEEE Trans. on Signal Processing*, Vol. 44, No. 11, 2757-2767, Nov. 1996.
7. Yu S.-J. and J.-H. Lee, "Adaptive array beamforming for cyclostationary signals," *IEEE Trans. on Antennas and Propagat.*, Vol. 44, No. 7, 943-953, Jul. 1996.
8. Lee, J.-H. and Y.-T. Lee, "Robust adaptive array beamforming for cyclostationary signals under cycle frequency error," *IEEE Trans. on Antennas and Propagat.*, Vol. 47, No. 2, 233-241, Feb. 1999.
9. Lee, J.-H., Y.-T. Lee, and W.-H. Shih, "Efficient robust adaptive beamforming for cyclostationary signals," *IEEE Trans. on Signal Processing*, Vol. 48, No. 7, 1893-1901, Jul. 2000.
10. Tang, H., K. M. Wong, A. B. Gershman, and S. Vorobyov, "Blind adaptive beamforming for cyclostationary signals with robustness against cycle frequency mismatch," *Proc. of IEEE Sensor Array and Multichannel Signal Processing Workshop*, 18-22, Rosslyn, VA, USA, Aug. 2002.

11. Vorobyov, S. A., A. B. Gershman, and Z.-Q. Luo, "Robust adaptive beamforming using worst-case performance optimization: A solution to the signal mismatch problem," *IEEE Trans. on Signal Processing*, Vol. 51, No. 2, 313–324, Feb. 2003.
12. Gardner, W. A., *Statistical Spectral Analysis: A Nonprobabilistic Theory*, Prentice Hall, Englewood Cliffs, NJ, 1988.
13. Gardner, W. A., "Exploitation of spectral redundancy in cyclostationary signals," *IEEE Signal Processing Mag.*, 14–36, Apr. 1991.
14. Wang, Z. and P. Stoica, "On robust Capon beamforming and diagonal loading," *IEEE Trans. on Signal Processing*, Vol. 51, No. 7, 1702–1715, Jul. 2003.
15. Lee, Y.-T. and J.-H. Lee, "Robust adaptive array beamforming with random error in cycle frequency," *IEE Proc. Radar, Sonar and Navigation*, Vol. 148, 193–199, Aug. 2001.
16. Lin, D., J. Li, and P. Stoica, "Fully automatic computation of diagonal loading levels for robust adaptive beamforming," *IEEE Trans. on Aerospace and Electronic Systems*, Vol. 46, No. 1, 449–458, Jan. 2010.
17. Li, Y., Y.-J. Gu, Z.-G. Shi, and K. S. Chen, "Robust adaptive beamforming based on particle filter with noise unknown," *Progress In Electromagnetics Research*, Vol. 90, 151–169, 2009.
18. Mallipeddi, R., J. P. Lie, P. N. Suganthan, S. G. Razul, and C. M. S. See, "Near optimal robust adaptive beamforming approach based on evolutionary algorithm," *Progress In Electromagnetics Research B*, Vol. 29, 157–174, 2011.
19. Mallipeddi, R., J. P. Lie, S. G. Razul, P. N. Suganthan, and C. M. S. See, "Robust adaptive beamforming based on covariance matrix reconstruction for look direction mismatch," *Progress In Electromagnetics Research Letters*, Vol. 25, 37–46, 2011.
20. Lee, J.-H., G.-W. Jung, and W.-C. Tsai, "Antenna array beamforming in the presence of spatial information uncertainties," *Progress In Electromagnetics Research B*, Vol. 31, 139–156, 2011.